Relationship between tremor and volcanic activity during the Southeast Crater eruption on Mount Etna in early 2000

Salvatore Alparone, Daniele Andronico, Luigi Lodato, and Tiziana Sgroi
Istituto Nazionale di Geofisica e Vulcanologia, Sezione di Catania, Catania, Italy

Received 8 March 2002; revised 14 October 2002; accepted 3 February 2003; published 13 May 2003.

[1] The Southeast Crater of Mount Etna (Italy) was characterized by a violent eruptive activity between 26 January and 24 June 2000. This activity produced 64 lava fountain episodes with repose periods from 3 hours to 10 days. We estimated a volume of about $15-20 \times 10^6$ m^3 lava and at least $2-3 \times 10^6$ m^3 of tephra. We compared the paroxysmal volcanic activity to its associated seismic signature: The high number of events highlighted a strict correlation between tremor and volcanic activity. Seismic and volcanic characteristics, such as the frequency of occurrence, the duration of lava fountains and the associated tremor energy, suggested the subdivision of the studied period into two stages separated by the 20 February event. Combining volcanic with seismic data, we observed some useful relationships among lava fountain height, sustained column height and Reduced Displacement; in addition, we found that the entire episode was well correlated with the duration of the amplitude increase. Computing the tremor energy linked to each event, the total energy associated with lava fountains episodes results in 76% of the energy released during the whole period. Finally, the different ratios among the overall spectral amplitude of the seismic signals of the stations located at different altitudes suggested to us the elaboration of a simple qualitative model to explain the dynamic behavior of the tremor source during the whole episode. *INDEX TERMS:* 7280 Seismology: Volcano seismology (8419); 8419 Volcanology: Eruption monitoring (7280); 8414 Volcanology: Eruption mechanisms; *KEYWORDS:* Mount Etna, lava fountain, volcanic tremor

Citation: Alparone, S., D. Andronico, L. Lodato, and T. Sgroi, Relationship between tremor and volcanic activity during the Southeast Crater eruption on Mount Etna in early 2000, *J. Geophys. Res.*, *108*(B5), 2241, doi:10.1029/2002JB001866, 2003.

1. Introduction

[2] Volcanic monitoring allows us to assess the status of active volcanoes. In fact, eruptions are usually preceded by a series of precursory phenomena, due to the rising of magma toward the surface, which produces considerable chemical and physical variations; the continuous measurements and the study of these parameters can strongly support the comprehension of eruption mechanisms.

[3] Seismic monitoring is considered the most favorable technique [*Swanson*, 1989]. In the past, the study of seismic activity (volcanic tremor and earthquakes) contributed to quite successfully forecast large explosive eruptions, such as Mount St. Helens in the United States in 1980, but more particularly in 1981–1982 during the following eruptive events [*Malone et al.*, 1983; *Swanson et al.*, 1983] and El Chicon in Mexico in 1982 [*Luhr and Varekamp*, 1984]. If we take only the variation in volcanic tremor amplitude into consideration, it presents bigger difficulties, such as at Hawaii, where it gave only a 50% success rate in prediction [*Klein*, 1982], whereas in some cases it gave an early warning together with the variation of other parameters, such as at Mount Etna in Italy in 1983 [*Cosentino et al.*, 1986] or at Redoubt in Alaska (USA) in 1989–1990 [*Page et al.*, 1994].

[4] Mount Etna, one of the best monitored volcanoes in the world, has four active craters located on the summit area (Figure 1). The Southeast Crater (SEC) has been the most active crater in the last 5 years, with an intense, almost continuous Strombolian activity, together with the emission of small lava flows. In the last few years, we have observed a strict correlation between tremor and eruptions [*Alparone and Privitera*, 2001]; tremor energy and the amplitude of certain frequency peaks usually change according to volcanic activity [*Falsaperla et al.*, 1994]. Although in the past research has been conducted on volcanic tremor to develop a seismic source model [*Seidl et al.*, 1981], detailed correlation analyses between tremor and volcanic activity are less frequent.

[5] On 26 January 2000, the SEC reactivated after about 3 months of quiescence. 64 lava fountain episodes occurred until 24 June, often preceded and usually followed by lava flows, and interspersed with periods of total or partial rest [*Quattrocchi et al.*, 2001]. This activity has been defined as "the SEC eruption in early 2000." In order to better understand the physics of explosive phenomena, we compared the observed paroxysmal volcanic activity (recorded by a video camera and acquired by visual observations)

0148-0227/03/2002JB001866$09.00

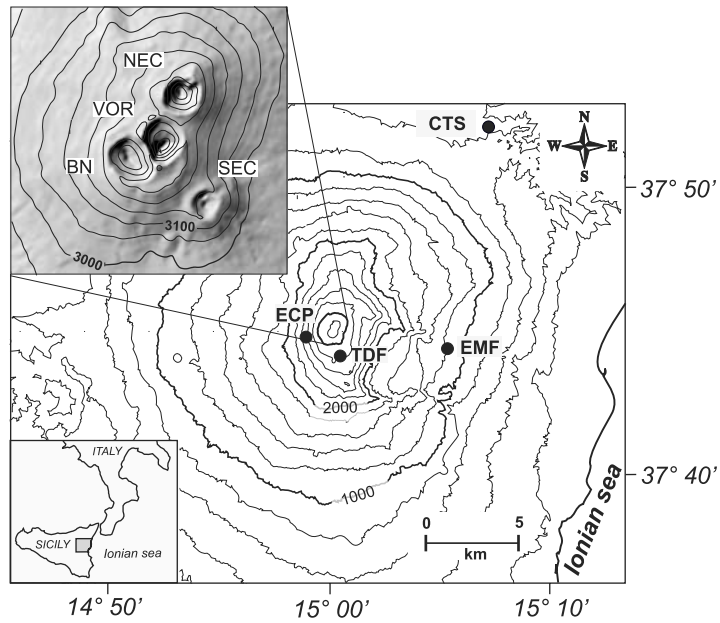

Figure 1. Map of Mount Etna volcano and location of the seismic stations used in the present work; contour interval is 200 m. The higher inset shows the map of summit craters. NEC = Northeast Crater, VOR = Voragine, BN = Bocca Nuova, SEC = Southeast Crater.

[e.g., *Pecora and Coltelli*, 2001] with its associated seismic signal.

[6] During the first six months of 2000, the pattern of volcanic tremor strongly reflected the evolution of the eruptive activity at SEC. The systematic relationship between the uprising of magma, the initialization of the eruptive episode and the increase in tremor amplitude, suggest that tremor may be used to better define the dynamics and evolution of lava fountains.

[7] Finally, the tremor pattern has also been very important as a precursor of fire-fountains at Etna. In fact, during the eruptive period we improved the accuracy of short-term predictions of fire-fountains, giving a less than 1 to 5 hour early warning before the eruption climax for 86% of them starting from 15 May [*Alparone et al.*, 2001; S. Alparone et al., INGV internal report, 2001].

2. Volcanic Tremor

[8] Active volcanoes are sources of seismic signals [*Malone*, 1983; *Gordeev et al.*, 1990]; among these, volcanic tremor represents an important phenomenology, because of its strict relationship with eruptive mechanisms [*Dibble*, 1974; *Aki et al.*, 1977; *Fehler and Chouet*, 1982; *Hofstetter and Malone*, 1986; *Chouet et al.*, 1987; *Koyanagi et al.*, 1987; *Page et al.*, 1994; *Julian*, 1994; *McNutt*, 1994; *Benoit and McNutt*, 1997]. Volcanic tremor has been studied at least on 160 volcanoes around the world [*Minakami*, 1960; *Fehler*, 1983; *McNutt*, 1994], suggesting distinct characteristics for each volcano, due to different volcanic activity and geometric and structural features. Many authors have discussed possible source mechanisms [*Gordeev*, 1993; *Julian*, 1994; *Benoit and McNutt*, 1997] and many models have been proposed [*Steinberg and Steinberg*, 1975; *Aki et al.*, 1977; *Chouet*, 1985, 1986; *Crosson and Bame*, 1985]. Some models consist of free oscillations of a magma chamber [*Sassa*, 1935; *Shima*, 1958; *Kubotera*, 1974]; oscillations of gas in a volcanic vent [*Steinberg and Steinberg*, 1975]; oscillations of volcanic layers from moving magma [*Omer*, 1950] and random opening of tensile cracks due to an excess of fluid pressures [*Aki et al.*, 1977; *Aki and Koyanagi*, 1981; *Chouet*, 1981].

[9] Mount Etna has been regularly monitored since 1971 and volcanic tremor studies date back some decades. They are focused on the tremor source [*Schick and Riuscetti*, 1973; *Riuscetti et al.*, 1977; *Seidl et al.*, 1981; *Schick et al.*, 1982; *Ferrucci et al.*, 1990; *Del Pezzo et al.*, 1993], spectral features [*Schick et al.*, 1982; *Falsaperla et al.*, 1994], wavefield polarizations [*Ferrucci et al.*, 1990; *Del Pezzo et al.*, 1993] and relationships with volcanic activity [*Tanguy and Patanè*, 1984; *Cosentino et al.*, 1989; *Gresta et al.*, 1991, 1996a, 1996b; *Falsaperla et al.*, 1994]. Many studies attribute the tremor source to pressure fluctuations derived from an unsteady magma flow and many models have been proposed [*Schick and Riuscetti*, 1973; *Riuscetti et al.*, 1977; *Seidl et al.*, 1981; *Schick*, 1981]. In detail, *Schick and Riuscetti* [1973] proposed that tremor energy could be associated with the velocity of gases escaping through the summit crater conduits, and the observed steadiness of the frequency peaks was related to at least one oscillator, excited by gas bubbles rising in the magma [*Riuscetti et al.*, 1977]. A physical model for the source was then proposed [*Seidl et al.*, 1981], and oscillators were identified with pipes along which magma rises.

[10] Many authors took into consideration the issue of the tremor source location at Etna. In particular, *Schick and Riuscetti* [1973] used amplitude-distance functions: results from several profiles in 1971 and 1972 showed a possible migration of the tremor source toward the northern part of the Valle del Bove (a large depression located on the eastern flank of the volcano) at a depth ranging from 2 to 4 km. *Riuscetti et al.* [1977] found two tremor sources below the Central Crater: a deeper source was located in the column, at a depth ranging from 0.5 to 1 km, and the other one on the free surface. Also *Schick et al.* [1982] distinguished two different sources: one was located in a magma chamber, 2 km below the Central Crater; the second one was associated with the upper portion of the active vents. Recently, *La Delfa et al.* [2001] discussed the violent outbursts at the SEC occurring between September 1998 and February 1999; also using tremor data, they proposed inferences on eruptive mechanisms based on cyclic replenishment of a shallow magma chamber.

[11] During the following years, array studies were carried out to resolve some of the problems concerning both tremor source location and wave propagation. Studying both amplitude and polarization patterns for major tremor episodes analyzed at the SEC during the 1989 eruption and using stations located near and far from the crater area, *Ferrucci et al.* [1990] suggested the existence of an elongated source having a horizontal projection trending north-south and radiating mainly *P* waves. Conversely, *Del Pezzo et al.* [1993] found a high content of surface waves originating from a source located in the summit crater area, using cross-correlation techniques on data collected with reference to a small seismic array during non-eruptive stages. During explosive paroxysmal summit eruptions, *Gresta et al.* [1996a] invoked the existence of a significant energy contribution linked to a planar sub-vertical source. Finally, it is noteworthy that the tremor polarization at Mount Etna is not steady: *Napoli et al.* [1994] observed that just before the 1991 eruption the tremor amplitude increased and the wave polarization changed from body waves to surface waves; however, short (1 s) pulses (*P* waves) were recognized near the summit crater rim [*Ripepe et al.*, 2001].

3. SEC Eruption in Early 2000

3.1. Previous Activity

[12] The 2000 SEC eruption was preceded by some years of lively eruptive activity. In fact, after the long-term 1991–1993 Etna eruption [*Calvari et al.*, 1994], the SEC resumed in November 1996, consisting of a discontinuous Strombolian activity that alternated with intracrater lava flow effusions. An intracrater cone grew starting in July 1997, while lava filling the crater bottom often overflowed southeastward from the crater rim until 1998, when eruptive activity first decreased and then stopped abruptly a few days after a violent paroxysmal eruption at the Voragine (Figure 1) on 22 July. On 15 September 1998, an explosive eruptive period began, characterized by 21 violent paroxysmal episodes [*Alparone and Privitera*, 2001]. On 4 February 1999, it culminated: during the last event, a fissure opened on the eastern flank of the cone, starting a mainly effusive eruption that lasted until 12 November 1999, having broken off from a vigorous lava fountain episode on September 4. During the last weeks of this activity also the Bocca Nuova crater (Figure 1) resumed, producing a summit eruption from 17 October until 5 November 1999, characterized by continuous violent Strombolian activity and vigorous lava effusion.

3.2. General Features of the 2000 Eruption

[13] The eruptive activity between 26 January and 24 June 2000, consisting of 64 fire-fountain episodes (Table 1), constitutes both an exceptional and unique series of paroxysmals within a short time in the known eruptive history of Etna.

[14] During the eruption, we were able to map the large volume of lava flows by aerial photos and recurring field studies; on the whole, the total lava field was preliminarily estimated to be $15-20 \times 10^6$ m^3 (Figure 2). In addition, explosive activity dispersed a large volume of ash, lapilli, scoriae and bombs, producing a thick cover of pyroclastics within a radius of 1 km, entirely mantling the 1998–1999 lava flows, and partially covering the coeval 2000 lava flows. With regard to pyroclastic material produced by explosive activity, the high frequency of the episodes together with frequently snow-capped and bad weather conditions, didn't permit us to carry adequate field surveys to collect a sufficient number of tephra samples. Nevertheless, using values of volume calculated for some representative events, for the whole eruptive period we estimated a value of about $2-3 \times 10^6$ m^3, a volume very much less than the lava flow volume.

[15] Because of this exceptional eruptive activity, the SEC grew a minimum of 40 m and was subjected to deep morphological and structural modifications. Two radial fissures formed and cut the southern and northern flanks of SEC, the first of them ending with a spatter rampart gradually built up at the southern flank of the cone, the second one with a more complex structure, which was mainly lava formed, on the northward sector.

4. Seismic Data Analysis

[16] In 2000, Mount Etna was monitored by two permanent seismic networks managed by Istituto Internazionale di Vulcanologia (IIV) and Sistema Poseidon, now merged with the Section of Catania of the Istituto Nazionale di Geofisica e Vulcanologia. The two permanent seismic networks comprise more than 50 stations, deployed at an altitude approximately ranging from 200 m to 2900 m. Most of them are equipped with vertical seismometers, besides eight 3-component stations (two of which are digital) are available, too. Data of the IIV and Sistema Poseidon networks are recorded at a sampling rate of 100 Hz and 160 Hz, respectively. Signals are transmitted via telephone lines and/or radio to the data acquisition centers in Catania, where they are digitally archived way and directly recorded on paper. Moreover, the signals coming from four stations have been analyzed on line with specific software, which has been able to compute the RMS tremor amplitude over a time window of 1 minute.

[17] In this work we use signals derived from four stations, equipped with 1 Hz seismometer, located at a distance ranging between 900 m and 20 km ca. from the

Table 1. Chronological Table of the 64 Lava Fountain Episodes

Episode Index	Date	Start	Duration, min	Energy, 10^7 J
1	Jan 26	3.50	565	80.7
2	Jan 29	6.55	95	18.7
3	Feb 01	7.55	100	12.9
4	Feb 02	6.45	65	8.8
5	Feb 03	6.50	85	8.7
6	Feb 04	8.45	50	10.1
7	Feb 04	22.40	70	2.1
8	Feb 05	10.40	85	3.2
9	Feb 06	3.20	50	5.5
10	Feb 06	21.50	65	9.5
11	Feb 07	15.40	75	11.6
12	Feb 08	10.15	75	20.1
13	Feb 08	18.55	70	6.0
14	Feb 09	6.50	65	8.0
15	Feb 09	23.20	35	7.9
16	Feb 10	12.10	55	12.4
17	Feb 11	4.25	55	14.2
18	Feb 11	20.45	60	17.1
19	Feb 12	2.50	70	12.3
20	Feb 12	8.25	75	8.1
21	Feb 12	23.25	55	16.9
22	Feb 13	11.35	25	13.1
23	Feb 14	2.10	60	11.4
24	Feb 14	15.00	30	12.5
25	Feb 15	16.50	40	12.1
26	Feb 16	5.40	25	10.7
27	Feb 16	15.05	20	7.4
28	Feb 17	4.00	25	9.3
29	Feb 17	12.05	25	9.1
30	Feb 17	20.30	25	9.2
31	Feb 18	6.40	20	11.4
32	Feb 18	15.35	20	9.5
33	Feb 19	7.55	45	15.6
34	Feb 20	3.00	45	21.2
35	Feb 20	15.45	90	16.2
36	Feb 23	2.30	105	37.1
37	Feb 27	6.40	165	55.4
38	Feb 28	14.55	100	14.9
39	Mar 04	1.45	120	53.0
40	Mar 08	6.35	145	91.0
41	Mar 12	11.35	130	4.0
42	Mar 14	5.50	125	3.3
43	Mar 19	0.10	115	15.1
44	Mar 22	18.15	125	17.5
45	Mar 24	18.30	95	16.9
46	Mar 29	19.00	115	13.8
47	Apr 01	7.40	180	83.6
48	Apr 03	12.30	165	75.0
49	Apr 06	9.50	105	58.5
50	Apr 16	9.20	215	145.0
51	Apr 26	4.15	80	65.9
52	May 05	11.50	370	112.0
53	May 15	9.00	60	45.7
54	May 15	20.35	90	38.0
55	May 17	21.05	125	29.2
56	May 19	21.25	115	58.6
57	May 23	1.40	115	42.4
58	May 27	18.30	195	46.3
59	Jun 01	0.45	500	93.0
60	Jun 01	18.25	125	55.2
61	Jun 05	3.35	145	47.5
62	Jun 08	10.35	280	51.7
63	Jun 14	5.50	250	49.8
64	Jun 24	15.00	440	37.2

SEC (Figure 1). The choice of these stations is linked to the best signal to noise ratio, in order to analyze the characteristics of tremor not only during the paroxysms, but also throughout relatively quiet phases.

4.1. Reduced Displacement

[18] We reconstructed temporal progress of Reduced Displacement (RD) linked to volcanic tremor amplitude. We used EMF as reference station for computing the RD because it operated continuously during the first 6 months of 2000, allowing to follow the entire evolution of eruptive phenomena.

[19] A moving average, computed every 5 minutes during the phases of tremor increase and every hour during periods of low level of tremor amplitude, has been performed on data of amplitude. The length of the time series (182 days) allowed us to analyze in detail the period that preceded, accompanied and followed the eruptive activity. These data have been compared to the estimate of RD, which is the most common way of quantifying tremor intensity. We have applied the formula proposed by *Fehler* [1983] to estimate the RD from surface waves in the far field:

$$RD = \frac{A\sqrt{\lambda r}}{2\sqrt{2}M}$$

where A is the peak-to-peak amplitude, λ is the wavelength, r is the SEC–station distance, and M is the instrument magnification. The $2\sqrt{2}$ term corrects root mean square (RMS) amplitude. In this way, the formula takes into consideration the effects of geometric spreading, instrument magnification and RMS amplitude.

[20] In Figure 3 the pattern of RD from 1 January to 30 June is shown. Every increase in tremor amplitude, which appears clearly in an impulsive way above a low level of noise, corresponds to a fire-fountain episode. We assume that each episode starts exactly when the tremor amplitude exceeds, for at least 10 minutes, the maximum amplitude of noise level (Table 1). Because of the time occurrence of explosive events, it is possible to distinguish roughly two eruptive stages: the first one consists of eruptions that occur much more frequently, up to three episodes per day; the second one, which started at the end of the 20 February episode, presents a maximum interval of 10 days between two consecutive episodes (Figure 3). Moreover, temporal intervals, during which episodes show a cyclic occurrence,

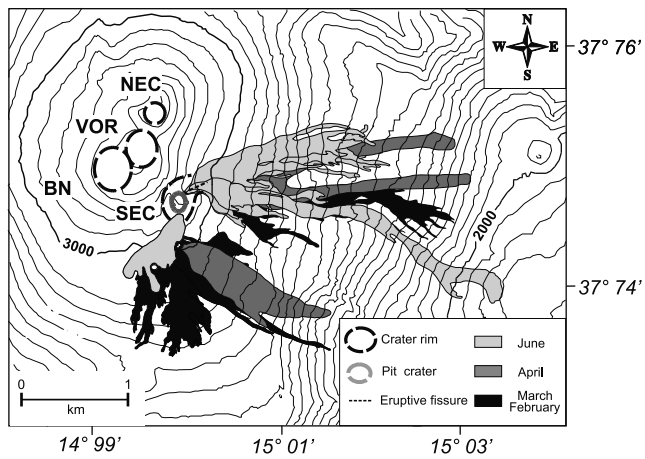

Figure 2. Map of the total lava field emitted during the eruption. Lava fields of January and May are hidden by the other lava flows.

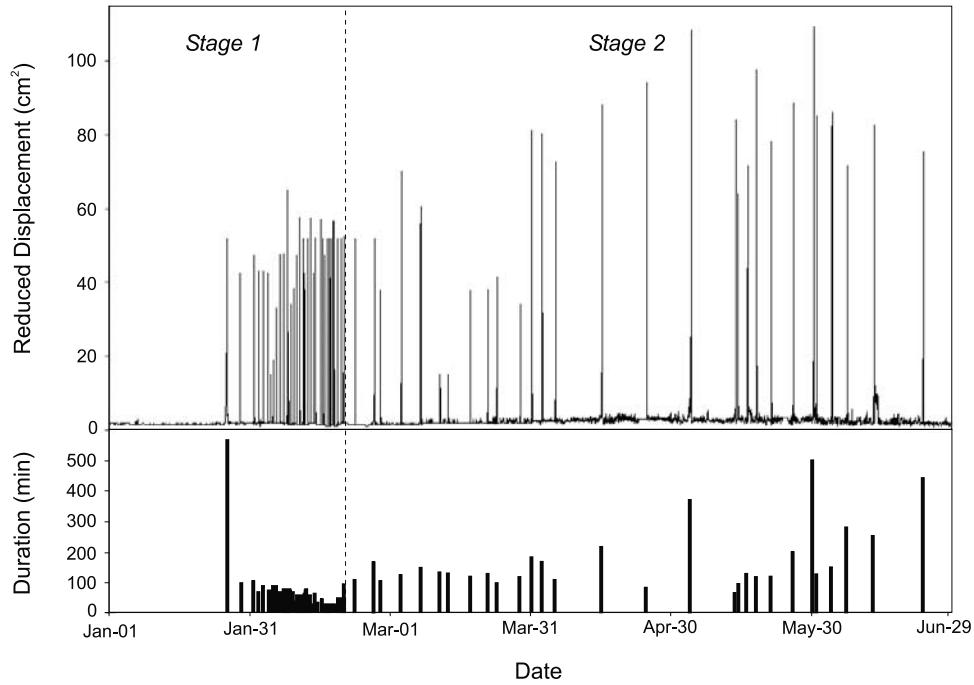

Figure 3. Top: Reduced Displacement pattern versus time during the period 1 January to 30 June. Bottom: duration of fountaining for each episode.

are recognized. In Figure 3, below the RD plot, a duration versus time diagram is shown. Except for the first episode (January 26), whose longer duration is probably associated with a revival of explosive activity, we can observe a pattern which confirms the distinction between two different stages: the first stage was characterized by a shorter duration of lava fountain, while the second one displays a higher average duration and a bigger variation in duration than the first one.

4.2. Energy Release

[21] We estimate the energy released from tremor episodes associated with eruptive phenomena starting from the seismic power [*Dibble*, 1974]:

$$P_T = \pi \rho_S v d^2 V^2$$

where $\rho_s = 2.5 \times 10^3$ kg/m^3 is the shallow-layer density as obtained by *Loddo et al.* [1989], v = 2.5 km/s is the average seismic wave velocity derived from studies of *Cristofolini et al.* [1987] and *Hirn et al.* [1991], d is the source-station distance (7.5 km), and V is the particle velocity at the station site, computed for the dominant frequency value of 1.76 Hz.

[22] To obtain the total energy radiated as tremor we consider the seismic power released in time (t):

$$E_T = t \times P_T$$

where t is expressed in seconds. Tremor energy has been computed from the previous equations for the whole studied period comprising both tremor amplitude increases and quiet periods.

[23] In Figure 4 the energy value related to the occurrence of the 64 lava fountain episodes is shown (see Table 1). The analysis of cumulative pattern of the energy demonstrates two different styles of energy release, characterized by different slopes, and confirms the subdivision of the eruption into the two above mentioned stages. The slope of the first period is higher than the second one. During the second

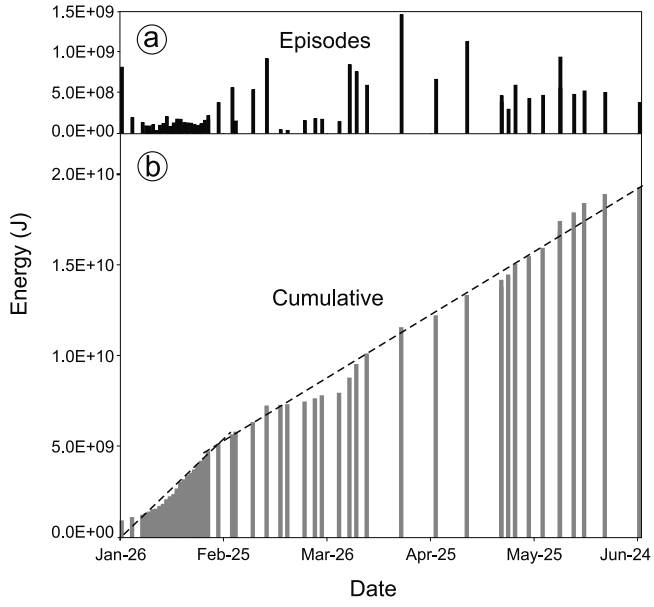

Figure 4. Evolution of the energy during the period 1 January to 30 June: (a) value of energy related to each episode of fountaining; (b) cumulative trend of the energy during the indicated period. This last diagram shows two well defined slopes, separated by the second event of 20 February.

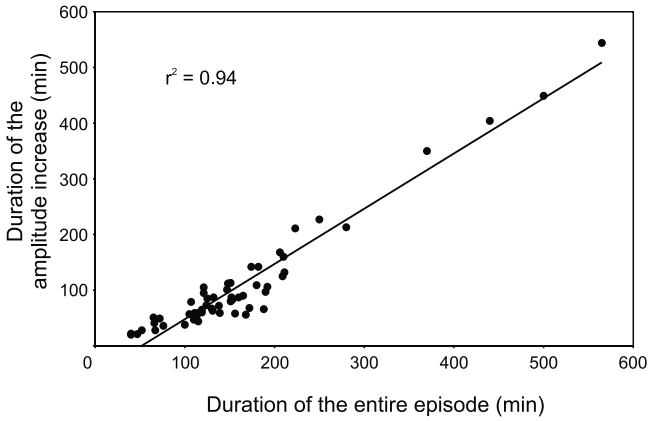

Figure 5. Increasing phase of amplitude tremor against whole duration of episode. A directly proportional relationship is well constrained and allows us to infer the end time of the fountaining during the paroxysmal phase.

period the slope does not substantially change until the end of the eruption, except for some fluctuations.

[24] The energy release as volcanic tremor concomitant with lava fountain episodes is about 76% of the total energy release in the whole period of activity, due to the recorded high tremor amplitudes during paroxysm episodes and a low background level between them.

4.3. Tremor Increase Versus Duration of the Episode

[25] We noticed a direct proportionality between the duration of a tremor increase phase (from the moment the episode starts to the maximum tremor amplitude) and the complete duration of the episode itself (the episode stopped when the recorded amplitude values revert to the values preceding the fountaining event) (Figure 5 and Table 1). The displayed pattern shows a low degree of scatter (r^2 = 0.94). This analysis and the achieved results are also important to forecast the duration of a lava fountain episode, which allows us to estimate the duration from the beginning phase.

4.4. Morphology

[26] The evolution of tremor amplitude versus time during each lava fountain episode allows us to recognize and classify three distinct and prevailing morphological patterns (Figure 6):

[27] ''Bell-shaped'' represents the prevalent type (47 examples) and is characterized by a gradual increase and decrease.

[28] ''Ramp-shaped'' presents a slow, gradual increase and a sudden decrease (9 cases).

[29] ''Tower-shaped'' shows a sudden increase and decrease (6 cases). The phase of most amplitude may be preceded by an initial ramp where tremor amplitudes increase slowly before the pattern assumes the typical ''tower-shape'' morphology. In particular, this kind of morphology characterized the last lava fountain episodes from the 23 May event. Only two events (on 1 February and 15 May) have shapes which were impossible to assign to these classes.

[30] Figure 6 shows the time sequence of lava fountain episodes associated with the relevant morphology. With the exception of the first three episodes, which we regard as belonging to a trigger phase of the eruption, the distribution of the morphologies also shows the main subdivision into

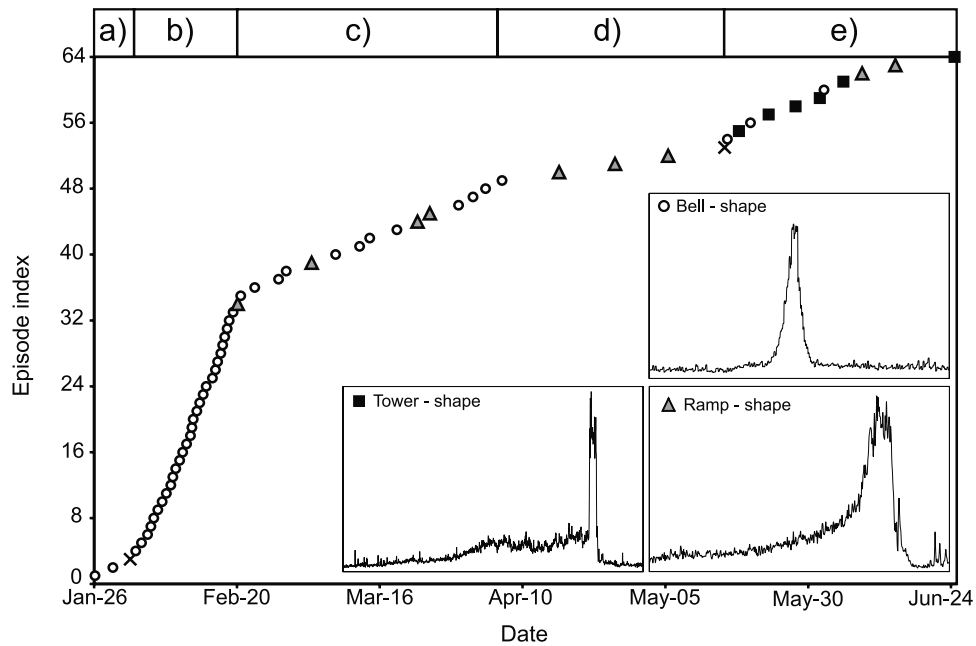

Figure 6. Diagram showing the evolution of 64 fountains from the morphologic seismic pattern point of view. We defined three main morphologies indicated with different symbols, with the exception of the 1 February and 15 May episodes (both indicated with X). We individuate five main portions: a) initial, formed by the three first events, b) ''bell'' regularly spaced, characterizing the first eruptive stage, c) cyclic (one or two ramp morphologies followed by four bell morphologies), d) wide spaced and e) irregular, during the final eruptive period.

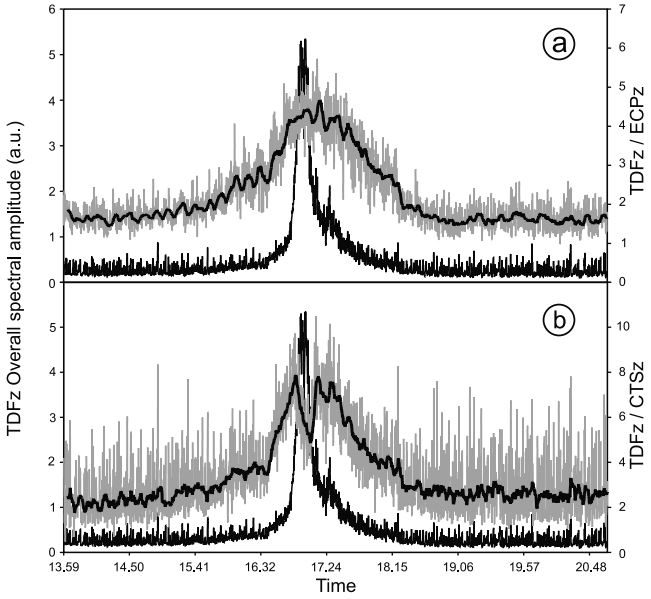

Figure 7. Ratios of the overall spectral amplitude recorded at TDF and ECP (the two considered summit stations) and CTS (the farther station). The thin dark line indicates the overall spectral amplitude, during the whole episode of lava fountain, recorded at TDF station; the gray line represents TDF/ECP (a) and TDF/CTS (b) ratios respectively. The thick dark line is the moving average of ratios which highlights the more significant variations.

the two above mentioned stages. In the whole series, we observed the predominance of the "bell-shape" and a particular distribution of the three morphological types. The bell-shape morphology is representative of the first stage (until 20 February); we noticed the first exception during the 1 February episode, when a change of slope was clearly recognizable ("b" in Figure 6). The first "ramp-shape" event precedes the opening of the fissure trending N-S at the base of the southern flank of the cone during the 23 February episode and is related to a new variation in the slope of the different morphologies distribution ("c" in Figure 6). During the second stage (20 February to 24 June), on the contrary, morphologies are more variable and characterized by a sharp cyclical occurrence.

[31] According to the morphological types and their temporal distribution, it is possible to subdivide the global trend of Figure 6 into five main portions: a) "initial" formed by the three first events, b) "regularly spaced bells" characterizing the first eruptive stage, c) "cyclic" (one or two ramp morphologies followed by four bell morphologies), d) "wide-spaced" and e) "irregular", relevant to the final eruptive period. So, a systematic regime is displayed, with well-defined patterns (b, c, and d portions), while in correspondence with portion "e" the system cannot maintain its equilibrium, showing strong irregularity in the distribution and in the characteristics of the episodes.

4.5. Amplitude Ratios

[32] Continuous spectral analyses were performed on the seismic signals recorded before, during and after the eruptive events. The spectral analyses were carried out using 10.24-second-long time windows by means of a Fast Fourier Transform algorithm; as a following step, overall spectral amplitude, defined as the cumulative of spectral amplitudes, was calculated in the frequency range from 0.01 to 10 Hz.

[33] In order to examine the spatial variation in the tremor source, we calculated the ratio of the overall spectral amplitude using seismic signals of stations located at different altitudes and distance from the summit area. In Figure 7 we report the most representative ratios, occurring between the seismic signals of two summit stations (TDF/ECP, Figure 7a) and of a summit station and the most peripheral one (TDF/CTS, Figure 7b; see also Figure 1 for their locations). According to *Gresta et al.* [1996a], we found significant fluctuations in the obtained plot. Before a lava fountain episode starts, the ratios of the overall spectral amplitudes are constant around the unity; then, in correspondence with the overall spectral amplitude increase (Strombolian activity, Figures 8 and 9), the tremor amplitude does not grow equally at each station, highlighting a variation in the ratio pattern which mainly depends on the different distance of each station from the tremor source.

[34] We analyzed the two ratios separately. Variations in the TDF/ECP ratio suggest that seismic source is nearer TDF station than ECP, as these stations are located at the same altitude (Figure 7a). During the maximum amplitude phase, the ratio reaches the highest values, returning to initial values at the end of episode. In general, the TDF/CTS ratio follows the same pattern too (Figure 7b), but during the paroxysmal phase it suffers an inversion, showing a marked decrease and reaching very low values. Taking into consideration that the station CTS is far from the crater area (about 18 km), the inversion of the ratio pattern suggests that, in this phase, the source is deeper.

5. Two Examples of Lava Fountains: The 29 March and 16 April Episodes

[35] Two examples show the variation in amplitude of volcanic tremor during lava fountain episodes, displaying a good correlation between the pattern of seismic tremor and the main variations of volcanic activity. In the following we imply Strombolian activity as a series of discrete magma bursts [*Blackburn et al.*, 1976]. At Etna the transition toward fountaining activity can be both gradual and, more often, sharp (as during the 2000 activity). Lava fountains usually consist of almost continuous to fully sustained, vigorous magma jets. To better define the eruptive sequence linked with the fire-fountaining, we subdivided each episode into three phases, according to the observed seismic and volcanic phenomena:

[36] 1. A "resumption phase," which often starts with a slow initial effusion from one or two vents along the two radial fissures, followed by a gradual increase in volcanic tremor amplitude, corresponding to increasing explosive activity.

[37] 2. A "paroxysmal phase," during which we observe a rapid transition from Strombolian activity to sustained lava fountains up to 800 m high. This phase usually lasts 10 to 60 minutes and is marked by a strong increase in effusive activity and frequent formation of a sustained column of ash, lapilli and steam (rising to 2–6 km), whose terminal region moves and disperses laterally producing a pyroclastic

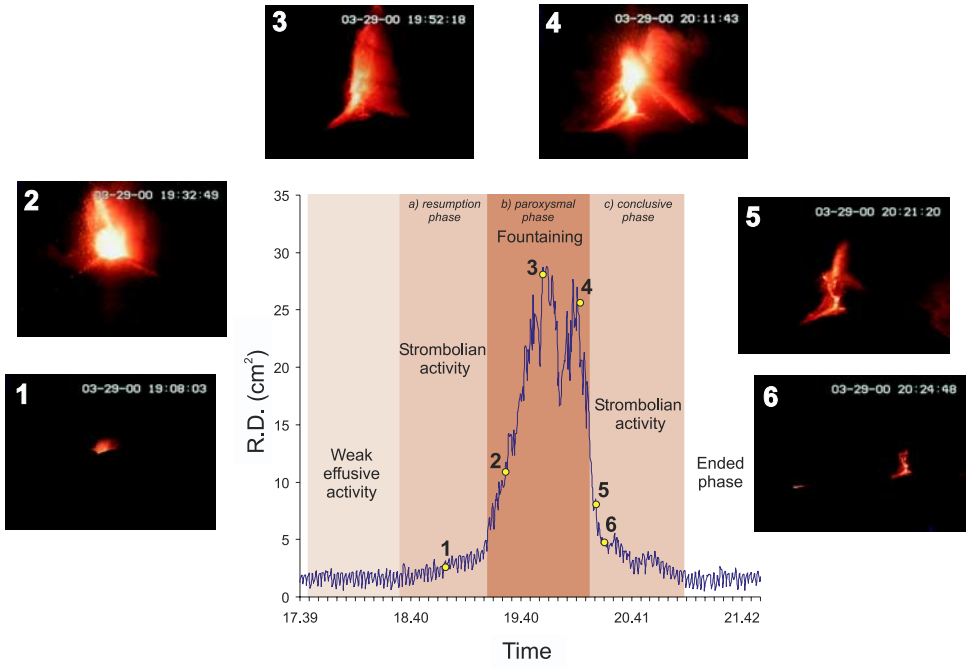

Figure 8. Comparison between volcanic tremor amplitude and video camera frames of the 29 March lava fountain episode. Volcanic phenomena are well correlated with the pattern of the seismic signature.

fallout downwind. The maximum tremor amplitudes were recorded during this phase.

[38] 3. A "conclusive phase," consisting of a marked drop in volcanic tremor, signaling the return to Strombolian activity before the cessation of the eruptive episode, corresponding to the re-establishment of the background tremor amplitude.

[39] We describe in detail one event occurring on 29 March 2000 (Figure 8). It represents the 46th episode since the eruptive period started on 26 January. The first explosion was observed at 18:09 (times are GMT), but beginning in the early afternoon a lava flow had been active along the northern fissure with no evidence of variation in the RD pattern. The explosive activity (Figure 8, frame 1) gradually increased until 19:21, when we recorded a mild increase in tremor amplitude. A more sudden increase in RD coincided with the transition from Strombolian activity to fountaining, with continuous jets of magma. The most violent paroxysmal phase occurred after 19:35 (Figure 8, frames 2 and 3), whereas a rootless lava flow formed and descended the cone from the southern rim until 19:38. The maximum tremor amplitude was reached at 19:55, after which the height of the fountain halved in no more than two minutes and the tremor markedly decreased in five minutes. It resumed briefly, due to low intensity fountaining starting at the spatter rampart built on the southward flank of the cone during the previous eruptive activity; the tremor seemed to be definitely decreasing after 20:11 (Figure 8, frame 4). At 20:15 the activity became Strombolian again, declining after 20:21 (Figure 8, frames 5 and 6).

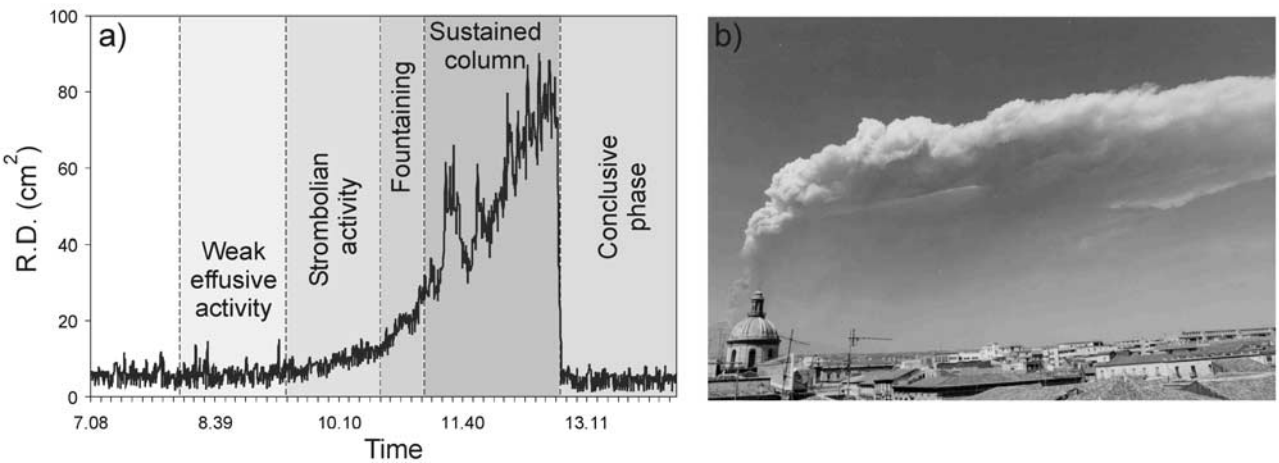

Figure 9. The 16 April lava fountain episode: (a) diagram of RD pattern and (b) photo of the eruptive plume taken from Catania.

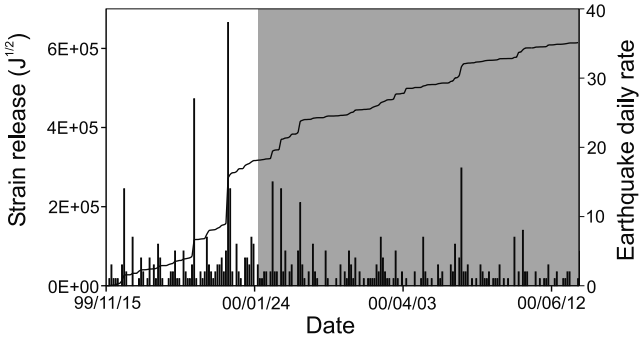

Figure 10. Cumulative strain release and number of earthquakes per day (Md $\geq$ 1.0) related to the period 15 November 1999 to 24 June 2000; the eruptive period is underlined in gray.

[40] The lava fountain on 16 April is probably the most spectacular explosive episode among all the 64 episodes and the one with the highest tremor energy release. It was characterized by a very long and complex paroxysmal phase (lasting 3.5 hours) and by the formation of a sustained column some tens of minutes after the start of fountaining, with a 2 to 6 km oscillating eruption plume over the cone (Figure 9). Like other lava fountains, the correspondence to the variations of RD was clear; at 12:30 we recorded the maximum amplitude, producing the ascent of the column up to 6 km, probably the highest observed during the whole eruption. This phase lasted until 12:51, when in concomitance with a marked decrease in tremor, the eruptive cloud was no longer sustained and the paroxysmal phase can be considered to have ended.

6. Discussion

6.1. Main Features of the Eruptive Period

[41] Volcanic tremor represents a powerful tool to study eruptive phenomena, allowing one to define and investigate eruptive mechanisms and processes of magma ascent. The uncommon activity of the year 2000 at SEC of Mount Etna and the high quality of data (improved in comparison to the past) provided an extraordinary opportunity to study short-lived events and assess a model of behavior of the volcano during fountaining activity. Our investigation at SEC gave evidence of a strict relation between tremor and impending volcanic phenomena when paroxysmal explosive activity occurred.

[42] During the first six months of 2000, an episodic eruption, characterized by a long succession of lava fountains (64 events), took place at SEC. From the seismic point of view, the eruption was not preceded by significant volcano-tectonic activity (Figure 10), dispersed all over the volcanic edifice, while the investigated period is characterized by a low level of seismicity, superimposed upon low energy swarms. We did not observe volcano-tectonic seismicity during the fountains; instead we recorded mainly high amplitude values of volcanic tremor signals and high values of energy release too. The seismic energy produced as tremor during the 64 fountains represents about 76% of total tremor amount; in the past *Carveni et al.* [1994] studied the three strongest explosive events of 1990 (5 and 15 January, and 1 February) and found total tremor energy release comparable to the usual yearly value [*Distefano and Gresta*, 1991].

[43] All seismic data we collected suggest different behavior of the volcano during the ongoing eruption, marked by the last lava fountain of 20 February, which allows us to subdivide the eruptive time span into two main stages. Using a frequency histogram representation, we noticed peculiar differences in repose time, energy, episode duration and maximum value of Reduced Displacement (RD_{max}) (Figure 11). In the first stage, lava fountains usually show a short repose time between episodes, a lower and roughly constant energy release, a well-defined RD_{max} class and a shorter duration time, while the fountaining events of the second stage show a wider variability. So, the first stage is characterized by a very rapid succession of fountains: 35 events in 26 days (from 26 January to 20 February), including also the first three more widely spaced episodes (Figure 4). In addition, lava fountain durations are clearly shorter up to the 35th episode, with the exception of the 26 January opening fountain and the following two events (Figure 3).

[44] These features reflect a variation of energy release after the 20 February episode, marked by a significant change in the eruptive dynamics during the 23 February episode, when a small active scar opened at the south base of the cone and closed at the end of April.

[45] From the volcanic point of view, the eruptive style of each episode remained constant throughout the studied period. In fact, during each episode of the eruptive activity we could always observe the three phases described above (“resumption” of explosive activity, “paroxysmal” phase with fountaining and often sustained column, and “conclusive” phase), associated with and nearly always preceded by the outpouring of lava flows. So, although the sequence of volcanic phenomena was comparable in both the first and in the second stages, duration (particularly of the paroxysmal phase) was greater in the second one. Secondarily, the increase of repose time between episodes is usually reflected in a longer lava effusion time before the following event. Furthermore, if the paroxysmal phase lasts longer, the eruptive episode will generally produce a larger amount of lava, higher volcanic plumes and, consequently, a wider distribution of scoria and ash fallout on the Etnean region.

6.2. Seismo-Volcanological Relations

[46] Table 2 shows all collected data concerning the maximum heights of both the jets of magma during the fountaining and, when they developed, the eruption columns; these data were collected by direct visual observations, photos and video images, using the height of the SEC as a scale. We do not have complete information about all episodes, mainly because of bad weather conditions in winter, particularly with reference to ejecta volume. In addition, some of these episodes occurred at night and we were not able to estimate the column height.

[47] Combining tremor with volcanic data, we achieved some important results. The main relations are reported in Figure 12. The greatest discrepancies inside the plots result from estimate errors, while in some cases they can be attributed to other variables which cannot be estimated, such as different eruptive dynamics. The fountaining activity, for example, can arise both from a conduit and along a fissure

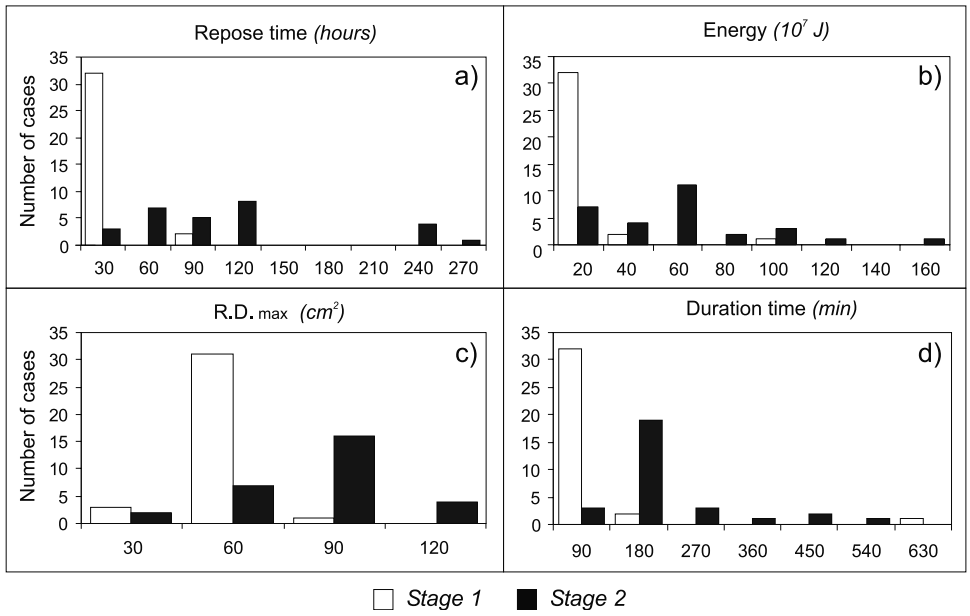

Figure 11. Histograms of selected parameters: (a) repose time; (b) energy; (c) RD_{max}; (d) duration time. We subdivided the two stages to enhance the more striking differences: white = first stage (26 January to 20 February), black = second stage (23 February to 24 June).

[*McNutt*, 1991], changing the initial eruptive conditions of each fountain. The 16 April event, that had a complex eruptive pattern, due to the coeval, highly intense activity at the southern spatter rampart (as described above), is representative of anomalies in our plots (Figure 12; circled point).

[48] There is a well-defined relation between "lava fountain height" and RD_{max} ($r^2 = 0.72$; Figure 12a); it stands to reason that higher fountains are associated with higher values of tremor, according also to *McNutt* [1991]. Also the "sustained column height" correlates reasonably well with the value of RD_{max} ($r^2 = 0.61$; Figure 12b); consequently, a good relationship between "lava fountain height" and "sustained column height" also occurs ($r^2 = 0.82$; Figure 12c). The relationships in Figure 12 between "lava fountain height", "sustained column height" and "RD_{max}" evidence some interdependence with each other: in fact high values of "RD_{max}" are usually associated with higher fountains and eruption plumes. Finally, Figure 12c suggests that "lava fountain height" versus "sustained column height" relation could be successfully used to forecast the potential height that a growing volcanic plume could reach during a fountaining episode.

[49] We tried to understand the importance of energy involved to constrain the evolution of volcanic phenomena, but unfortunately we didn't find satisfactory correlations, in particular in the comparison between "energy" with "lava fountain height" and "sustained column height". This is possible because a high quantity of energy can be released slowly, that is over a long time, without allowing the occurrence of violent paroxysmal. Again, we do not have a clear dependence of "duration time" of paroxysmals on "RD_{max}" or "lava flow volumes." We found only a partial proportional relationship for higher values of "repose time" occurring between lava fountain episodes versus "energy," "duration time" and "RD_{max}".

[50] In summary, comparing seismic and volcanic data we can draw some conclusions. During each lava fountain the height of magma jets and of sustained column is related to the "RD_{max}" recorded. Nevertheless, the same "RD_{max}" can be recorded during a wide range of fire-fountain durations, in which both short and long episodes can be characterized by the same value of tremor amplitude. Finally, we found no significant correlation among volume data related to lava flows emitted during paroxysmal phases with any other compared parameters.

6.3. Inferences About Eruptive Dynamics

[51] We obtained significant results, in terms of dynamics of the tremor source, from ratios of the overall spectral

Table 2. Summary of Lava Fountain and Sustained Column Height Values

Episode Index	Date	Fountain Height, m	Column Height, km
11	Feb 07	200	3.2
18	Feb 11	250/300	not visible
19	Feb 12	350/400	not visible
24	Feb 14	350/400	4
25	Feb 15	>500	not visible
27	Feb 16	300/350	>3
39	Mar 04	400	absent
40	Mar 08	300	3
41	Mar 12	80	not visible
42	Mar 14	200/250	not visible
44	Mar 22	300/350	not visible
46	Mar 29	400	absent
47	Apr 01	*fog*	3
49	Apr 06	300/350	absent
50	Apr 16	400	6
51	Apr 26	*no data*	5
52	May 05	800	4.5/5
54	May 15	700	not visible
55	May 17	500	not visible
59	Jun 01	800	5.5
61	Jun 05	500/600	4
63	Jun 14	600	4.5
64	Jun 24	500	3/4

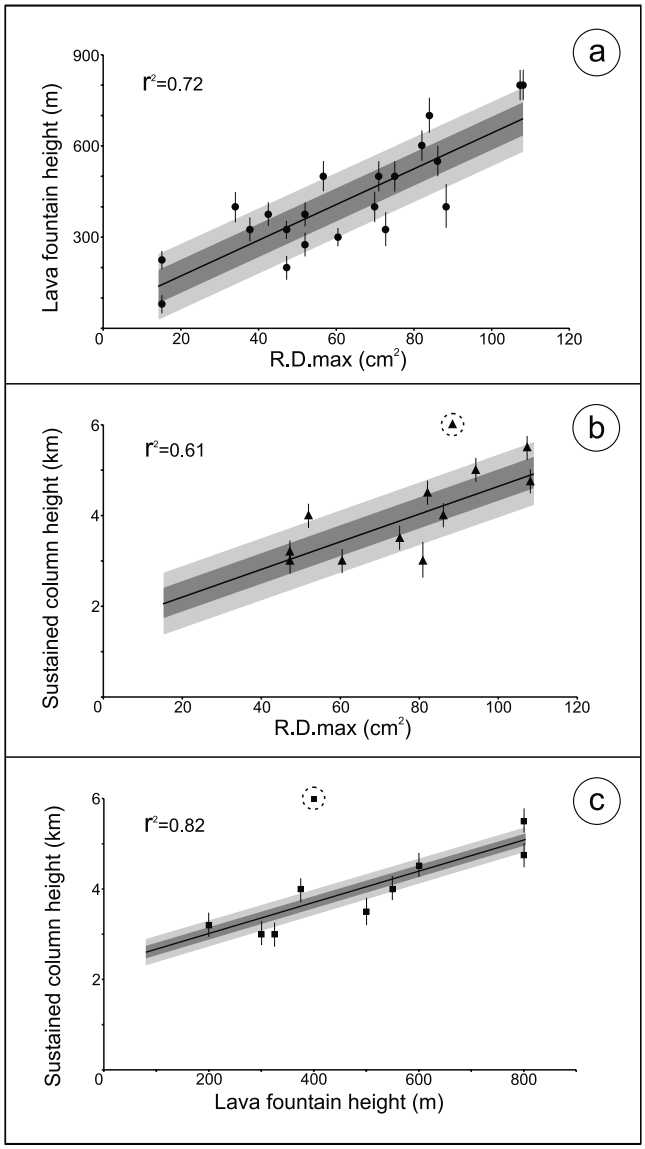

Figure 12. Comparison among lava fountain height, sustained column height and RD_{max}: (a) lava fountain height versus RD_{max}; (b) sustained column height versus RD_{max}; (c) sustained column height versus lava fountain height. All the diagrams show a good correspondence between data used, as confirmed by the r^2 values. We circled the 16 April anomalous lava fountain episode, not considered in the best fit line calculation (see text for explanation). The dark and light gray areas correspond to the 1σ and 2σ uncertainties respectively of the best fit line.

amplitudes of seismic signals recorded at different altitudes and distances from the summit (Figure 7). On the basis of our considerations, we have tried to offer a qualitative model to explain the observed pattern of the overall spectral amplitude and the relevant ratios.

[52] We think that the knowledge of the fluid-dynamic phenomena occurring in the volcanic apparatus is very important in the context of source modeling. We infer the presence of a seismic source linked to the "upper portion" of a small magma chamber located under the SEC. During the "*resumption phase*" of each lava fountain episode, the magma batch begins to fragment and exsolve gases. Movement, coalescence and migration of gas bubbles trigger the start of volcanic processes, while the seismic source of the tremor migrates slowly upward, giving a weak increase in the mean amplitude to stations closer to the summit area. During this phase the shallow magmatic portions are involved. Continuous gas exolution forms foam on the top of the magma column, whose expansion allows a gradual ascent of magma toward the surface along the volcanic conduit of the SEC. The occurrence of the first Strombolian bursts reveals that a new paroxysm is imminent.

[53] When the tremor source has almost reached the surface, the magma batch is subjected to a quick depressurization process: Strombolian explosions become more and more violent, finally changing to lava fountaining activity, while the seismic radiation indicates a marked energization. The continuous extraction of magma and the gradual emptying of the magma chamber allow the depressurization process to involve a deeper magma system. Consequently, in correspondence to the tremor maximum amplitude phase, the tremor source becomes deeper. The most peripheral seismic stations, located on the lowest part of volcano, feel the effects of the source deepening, which causes the trend described in Figure 7b in the tremor amplitude ratio.

7. Concluding Remarks

[54] The higher data quality (compared to the recent past) of the study of lava fountain episodes occurring during the SEC eruption on Mount Etna in early 2000, have allowed us to obtain the following significant results.

[55] 1. A good correspondence is found between volcanic activity and variation in tremor amplitude.

[56] 2. Identification of three different phases ("resumption," "paroxysmal" and "conclusive") during the majority of lava fountain episodes, each one characterized by a similar progression of eruptive and seismic phenomena.

[57] 3. Using different parameters such as energy, duration, morphologic pattern, etc., the January–June 2000 eruptive period at Etna has been defined, characterized and subdivided into at least two stages.

[58] 4. On the basis of morphology of tremor pattern of each lava fountain episode and its temporal distribution during the 26 January to 24 June period, we recognize five steps. We retain that the variation of some factors determining dynamics of lava fountains, e.g., the geometry of the volcanic system, the ascent rate of magma from depth up to the shallow chamber, the amount of gas in the uprising magma batches, produce such short eruptive "sub-periods."

[59] 5. Comparison between volcanic and seismic parameters allowed us to recognize some important relationships during the occurrence of each episode, such as duration of episodes, the height the lava fountain and/or the eruption columns reached.

[60] The close-up sequence of explosive short-lived events and the possibility to record variations in the tremor amplitudes at different seismic stations allowed us to define a general model concerning the dynamics of the source of tremor.

[61] The explosive activity of the "2000 eruption" at SEC consisted of periodic ascent of magma batches from a shallow

plumbing system, whose filling and subsequent emptying produced 64 lava fountain events. We infer the existence of a volcanic system (conduit plus magma chamber) which extends vertically under the SEC area. Dynamics of bubble gases inside this system produce variations in the location and extension of the tremor source. During the early phase of the lava fountain episode the source activates and migrates upward in the volcanic conduit, while in the paroxysmal phase it deepens, involving deeper magma portions of the shallow plumbing system and determining itself elongation. This qualitative model is consistent with the maintaining of a constant eruptive process that produces roughly similar seismic and volcanological dynamics for each episode.

[62] We suggest that all the observed relations could be successfully applied to assess future paroxysmal activity and improve the accuracy of short-term predictions. Consequently, we believe that our results are important in order to reduce the risk coming from explosive activity, which is relatively modest on the lower slopes but increases dramatically toward the top of volcano, due to the fact that, since the summit area of the volcano is a famous scientific and tourist attraction, both volcanologists and visitors are often exposed to volcanic risk.

[63] **Acknowledgments.** We wish to thank Stefano Gresta for his stimulating comments and suggestions, and Larry Mastin and an anonymous reviewer for constructive criticism. We are grateful to Letterio Villari, who first encouraged our research, and Eugenio Privitera for the help received in the discussion. We wish to thank also Sonia Calvari for her useful suggestions. This work was supported by INGV - Sezione di Catania.

References

Aki, K., M. Feheler, and S. Das, Source mechanism of volcanic tremor: Fluid-driven crack models and their application to the 1963 Kilauea eruption, *J. Volcanol. Geotherm. Res.*, *2*, 259–287, 1977.

Aki, K., and R. Koyanagi, Deep volcanic tremor and magma ascent mechanism under Kilauea, Hawaii, *J. Geophys. Res.*, *86*, 7095–7109, 1981.

Alparone, S. and E. Privitera, Characteristics of the intermittent volcanic tremor at Mt. Etna, Italy, during the 15 September 1998–4 February 1999 eruptive episode, in *Proceedings of the Cities on Volcanoes 2 Conference*, *Auckland, New Zealand, 12–14 February 2001, Earthquake Commission*, *Inst. Geol. Nucl. Sci. Inf. Ser.*, vol. 49, Inst. of Geol. and Nucl. Sci, Lower Hutt, New Zealand, 2001.

Alparone, S., D. Andronico, L. Lodato, and T. Sgroi, An approach to forecasting of paroxysmal eruptions at Mount Etna using the relationship between tremor and volcanic activity, in *Proceedings of the Cities on Volcanoes 2 Conference*, *Auckland, New Zealand, 12–14 February 2001, Earthquake Commission*, *Inst. Geol. Nucl. Sci. Inf. Ser.*, vol. 49, Inst. of Geol. and Nucl. Sci, Lower Hutt, New Zealand, 2001.

Benoit, J. P., and S. McNutt, New constraints on source processing of volcanic tremor at Arenal Volcano, Costa Rica, using broadband seismic data, *Geophys. Res. Lett.*, *24*, 449–452, 1997.

Blackburn, E. A., L. Wilson, and R. S. J. Sparks, Mechanism and dynamics of strombolian activity, *J. Geol. Soc. London*, *132*, 429–440, 1976.

Calvari, S., M. Coltelli, M. Neri, M. Pompilio, and V. Scribano, The 1991–1993 Etna eruption: Chronology and lava flow-field evolution, *Acta Vulcanol.*, *4*, 1–14, 1994.

Carveni, P., R. Romano, T. Catabiano, M. F. Grasso, and S. Gresta, The exceptional explosive activity of 5 January 1990 at the SE-Crater of Mt. Etna volcano (Sicily), *Boll. Soc. Geol. It.*, *113*, 613–631, 1994.

Chouet, B., Ground motion in the near field of a fluid-driven crack and its interpretation in the study of shallow volcanic tremor, *J. Geophys. Res.*, *86*, 5985–6016, 1981.

Chouet, B., Excitation of a buried magmatic pipe: a seismic source model for volcanic tremor, *J. Geophys. Res.*, *91*, 1881–1893, 1985.

Chouet, B., Dynamics of a fluid-driven crack in three dimensions by the finite difference method, *J. Geophys. Res.*, *91*, 1881–1893, 1986.

Chouet, B. A., R. Y. Koyanagi, and K. Aki, Origin of volcanic tremor in Hawaii, part II: Theory and discussion, in *Volcanism in Hawaii*, vol. 2, edited by R. W. Decker, T. L. Wright, and P. H. Stauffer, *U.S. Geol. Surv. Prof. Pap., 1350*, 1259–1280, 1987.

Cosentino, M., M. Di Francesco, G. Lombardo, and E. Privitera, Volcanic activity at Mt. Etna and possible seismological precursors, *Period. Mineral.*, *55*, 131–142, 1986.

Cosentino, M., G. Lombardo, and E. Privitera, A model for internal dynamical processes on Mt. Etna, *Geophys. J.*, *97*, 367–379, 1989.

Cristofolini, R., S. Gresta, S. Imposa, S. Menza, and G. Patanè, An approach to problems on energy sources at Mount Etna based on seismological and volcanological data, *Bull. Volcanol.*, *49*, 729–736, 1987.

Crosson, R. S., and D. A. Bame, A spherical source model for low frequency volcanic earthquakes, *J. Geophys. Res.*, *90*, 10,237–10,247, 1985.

Del Pezzo, E., S. De Martino, S. Gresta, M. Martini, G. Milana, D. Patanè, and C. Sabbarese, Velocity and spectral characteristics of the volcanic tremor at Etna deduced by a small seismometer array, *J. Volcanol. Geotherm. Res.*, *56*, 369–378, 1993.

Dibble, R. R., Volcanic seismology and accompanying activity of Ruapehu Volcano, New Zealand, in *Physical Volcanology*, edited by L. Civetta et al., pp. 49–85, Elsevier Sci., New York, 1974.

Distefano, G., and S. Gresta, Energy releases at Etna volcano during 1983–87, *Acta Vulcanol.*, *1*, 39–42, 1991.

Falsaperla, S., E. Privitera, S. Spampinato, and C. Cardaci, Seismic activity and volcanic tremor related to the December 14, 1991 Mt. Etna eruption, *Acta Vulcanol.*, *4*, 63–73, 1994.

Fehler, M., Observations of volcanic tremor at Mount S. Helens volcano, *J. Geophys. Res.*, *88*, 3476–3484, 1983.

Fehler, M., and B. A. Chouet, Operation of a digital seismic network on Mt. St. Helens volcano and observations of long-period seismic events that originate under the volcano, *Geophys. Res. Lett.*, *9*, 1017–1020, 1982.

Ferrucci, F., C. Godano, and N. A. Pino, Approach to the volcanic tremor by the covariance analysis: Application to the 1989 eruption of Mt. Etna (Sicily), *Geophys. Res. Lett.*, *17*, 2425–2428, 1990.

Gordeev, E., Modeling of volcanic tremor as explosive point sources in a single-layered, elastic half-space, *J. Geophys. Res.*, *98*, 19,687–19,703, 1993.

Gordeev, E. I., V. A. Saltykov, V. I. Siniysyn, and V. N. Chebrov, Temporal and spatial characteristics of volcanic tremor wave fields, *J. Volcanol. Geotherm. Res.*, *40*, 89–101, 1990.

Gresta, S., A. Montalto, and G. Patanè, Volcanic tremor at Mt. Etna (January 1984–March 1985): Its relationship to the eruptive activity and modelling of the summit feeding system, *Bull. Volcanol.*, *53*, 309–320, 1991.

Gresta, S., G. Lombardo, and R. Cristofolini, Characteristics of volcanic tremor accompanying the September 24th, 1986 explosive eruption of Mt. Etna (Italy), *Ann. Geofis.*, *39*, 411–421, 1996a.

Gresta, S., E. Privitera, A. Leotta, and P. Gasperini, Analysis of the intermittent volcanic tremor observed at Mount Etna (Sicily), during March–May 1987, *Ann. Geofis.*, *39*, 421–428, 1996b.

Hirn, A., A. Nercessian, M. Sapin, F. Ferrucci, and G. Wittlinger, Seismic heterogeneity of Mount Etna: structure and activity, *Geophys. J. G. Int.*, *105*, 139–153, 1991.

Hofstetter, A., and S. D. Malone, Observations of volcanic tremor at Mt. St. Helens in April and May 1980, *Bull. Seismol. Soc. Am.*, *76*, 923–938, 1986.

Julian, B. R., Volcanic tremor: non linear excitation by fluid flow, *J. Geophys. Res.*, *99*, 11,859–11,877, 1994.

Klein, F. W., Patterns of historical eruptions at Hawaiian volcanoes, *J. Volcanol. Geotherm. Res.*, *12*, 1–35, 1982.

Koyanagi, R. Y., B. A. Chouet, and K. Aki, Origin of volcanic tremor in Hawaii, part I: Data from the Hawaiian Volcano Observatory, 1969–1985, *U.S. Geol. Surv. Prof. Pap.*, *1350*, 1221–1258, 1987.

Kubotera, A., Volcanic tremors at Aso volcano, *Dev. Solid Earth Geophys.*, *6*, 29–47, 1974.

La Delfa, S., G. Patanè, R. Clocchiatti, J.-L. Joron, and J.-C. Tanguy, Activity of Mount Etna preceding the February 1999 fissure eruption: Inferred mechanism from seismological and geochemical data, *J. Volcanol. Geotherm. Res.*, *105*, 121–139, 1999.

Loddo, M., D. Patella, R. Quarto, G. Ruina, A. Tramacere, and G. Zito, Application of gravity and deep dipole geoelectrics in the volcanic area of Mount Etna (Sicily), *J. Volcanol. Geotherm. Res.*, *39*, 17–39, 1989.

Luhr, J. F., and J. C. Varekamp (Eds.), El Chicon volcano, Chiapas, Mexico, *J. Volcanol. Geotherm. Res.*, *Spec. Issue 23*, 191 pp., 1984.

Malone, D. S., C. Boyko, and C. S. Weaver, Seismic precursor to the Mount St. Helens eruptions 1981–1982, *Science*, *221*(4618), 1376–1378, 1983.

Malone, S., Volcanic Earthquakes: Examples from Mount St. Helens, in *Earthquakes*: *Observations, Theory and Interpretation*, edited by H. Kanamori and E. Boschi, pp. 436–455, Elsevier Sci., New York, 1983.

McNutt, S. R., Volcanic tremor, in *Encyclopedia of Earth System Science*, vol. 4, p. 9, Academic, San Diego, Calif., 1991.

McNutt, S. R., Volcanic tremor from around the world: 1992 update, *Acta Vulcanol.*, *5*, 197–200, 1994.

Minakami, T., Earthquakes and crustan deformation originating from volcanic activities, *Bull. Earthquake Res. Inst.*, *38*, 497–544, 1960.

Napoli, R., F. Ferrucci, and S. Gresta, Polarisation of tremor wave field at Mt. Etna Volcano and some open question on type and dynamics of the source: Comparison between 1989 and 1991–1993 eruptions, *Acta Volcanol.*, *4*, 57–61, 1994.

Omer, G. C., Volcanic tremor, *Bull. Seismol. Soc. Am.*, *40*, 175–194, 1950.

Page, R. A., J. C. Lahr, B. A. Chouet, J. A. Power, and C. D. Stephens, Statistical forecasting of repetitious dome failures during the waning eruption of Redoubt Volcano, Alaska, February–April 1990, *J. Volcanol. Geotherm. Res.*, *62*, 183–196, 1994.

Pecora, E., and M. Coltelli, Studio della correlazione tra il tremore vulcanico e l'attività esplosiva dell'Etna nel gennaio-febbraio 1999 mediante il sistema VoTA (Volcanic Tremor Analizer), *INGV Internal Rep. 246/02*, pp. 1–14, Ist. Naz. di Geofis. e Vulcanol., Catania, Italy, 2001.

Quattrocchi, F., G. Di Stefano, G. Galli, L. Pizzino, P. Scarlato, P. Allard, D. Andronico, D. Condarelli, and T. Sgroi, Water-rock interactions during seismic and volcanic activity recorded at Mount Etna by continuous groundwater monitoring, in *Water-Rock Interaction*, edited by R. Cidu, pp. 107–110, A. A. Balkema, Brookfield, Vt., 2001.

Ripepe, M., M. Coltelli, E. Privitera, S. Gresta, M. Moretti, and D. Piccinini, Seismic and infrasonic evidences for an impulsive source of the shallow volcanic tremor at Mt. Etna, Italy, *Geophys. Res. Lett.*, *28*, 1071–1074, 2001.

Riuscetti, M., R. Schick, and D. Seidl, Spectral parameters of volcanic tremor at Etna, *J. Volcanol. Geotherm. Res.*, *2*, 289–298, 1977.

Sassa, K., Volcanic micro-tremor and eruption earthquakes, *Mem. Coll. Sci. Univ. Kyoto.*, *18*, 255–293, 1935.

Schick, R., Source mechanism of volcanic tremor, *Bull. Volcanol.*, *44*, 491–497, 1981.

Schick, R., and M. Riuscetti, An analysis of volcanic tremor at South-Italian volcanoes, *Z. Geophys.*, *39*, 262–274, 1973.

Schick, R., M. Cosentino, G. Lombardo, and G. Patanè, Volcanic tremor at Mt. Etna: A brief description, *Mem. Soc. Geol. It.*, *23*, 191–196, 1982.

Seidl, D., R. Schick, and M. Riuscetti, Volcanic tremors at Etna: a model for hydraulic origin, *Bull. Volcanol.*, *44*, 43–56, 1981.

Shima, M., On the second volcanic microtremor at volcano Aso, *Bull. Disaster Prev. Res.*, *19*, 11–56, 1958.

Steinberg, G. S., and A. S. Steinberg, On possible causes of volcanic tremor, *J. Geophys. Res.*, *80*, 1600–1604, 1975.

Swanson, D. A., Can one foresee volcanic eruptions? A personal perspective, in *Proceedings of the International Conference: Sono prevedibili i terremoti e le eruzioni vulcaniche?*, Presidenza del Consiglio dei Ministri, Taormina, Italy, 1989.

Swanson, D. A., T. J. Casadevall, D. Dzurisin, S. D. Malone, C. G. Newhall, and C. S. Weaver, Predicting eruptions at Mount St. Helens, June 1980 through December 1982, *Science*, *221*(4618), 1369–1376, 1983.

Tanguy, J. C., and G. Patanè, Activity of Mount Etna 1977–1983: Volcanic phenomena and accompanying seismic tremor, *Bull. Volcanol.*, *47*, 965–976, 1984.

S. Alparone, D. Andronico, L. Lodato, and T. Sgroi, Istituto Nazionale di Geofisica e Vulcanologia, Sezione di Catania, Catania, Italy.